Published in final edited form as:
J Appl Microbiol. 2012 October ; 113(4): 940–951. doi:10.1111/j.1365-2672.2012.05337.x.

Cell surface hydrophobicity of colistin-susceptible *versus* -resistant *Acinetobacter baumannii* determined by contact angles: methodological considerations and implications

Rachel L. Soon[1], **Jian Li**[1], **John D. Boyce**[2,3], **Marina Harper**[2,3], **Ben Adler**[2,3], **Ian Larson**[1,*], and **Roger L. Nation**[1,#,*]

[1]Facility for Anti-infective Drug Development and Innovation, Drug Delivery, Disposition and Dynamics, Monash Institute of Pharmaceutical Sciences, Monash University, 381 Royal Parade, Parkville 3052, Victoria, Australia

[2]Department of Microbiology, Monash University, Victoria, Australia

[3]Australian Research Council Centre of Excellence in Structural and Functional Microbial Genomics, Monash University, Victoria, Australia

Abstract

AIMS—Contact angle analysis of cell surface hydrophobicity (CSH) describes the tendency of a water droplet to spread across a lawn of filtered bacterial cells. Colistin-induced disruption of the Gram-negative outer membrane necessitates hydrophobic contacts with lipopolysaccharide (LPS). We aimed to characterize the CSH of *Acinetobacter baumannii* using contact angles, to provide insight into the mechanism of colistin resistance.

METHODS AND RESULTS—Contact angles were analysed for five paired colistin-susceptible and -resistant *A. baumannii* strains. Drainage of the water droplet through bacterial layers was demonstrated to influence results. Consequently, measurements were performed 0.66-sec after droplet deposition. Colistin-resistant cells exhibited lower contact angles (38.8±2.8° to 46.8±1.3°) compared to their paired-susceptible strains (40.7±3.0° to 48.0±1.4°; *ANOVA; p*<0.05). Contact angles increased at stationary phase (50.3±2.9° to 61.5±2.5° and 47.4±2.0° to 50.8±3.2°, susceptible and resistant, respectively, *ANOVA; p*<0.05), and in response to colistin 32-mgL^{-1} exposure (44.5±1.5° to 50.6±2.8° and 43.5±2.2° to 48.0±2.2°, susceptible and resistant, respectively; *ANOVA; p*<0.05). Analysis of complemented strains constructed with an intact *lpxA* gene, or empty vector, highlighted the contribution of LPS to CSH.

CONCLUSIONS—Compositional outer-membrane variations likely account for CSH differences between *A. baumannii* phenotypes, which influence the hydrophobic colistin-bacterium interaction.

SIGNIFICANCE AND IMPACT OF STUDY—Important insight into the mechanism of colistin resistance has been provided. Greater consideration of contact angle mehodology is nescessary to ensure accurate analyses are performed.

Keywords

Antimicrobials; Lipopolysaccharide; Mechanism of Action

[#]Corresponding author. Facility for Anti-infective Drug Development and Innovation, Drug Delivery, Disposition and Dynamics, Monash Institute of Pharmaceutical Sciences, Monash University, 381 Royal Parade, Parkville, Victoria 3052, Australia. Phone: +61 3 9903 9061. Fax: +61 3 9903 9629. Roger.Nation@monash.edu.
[*]Joint senior authors contributed equally to this work.

Introduction

Multidrug-resistant (MDR) Gram-negative pathogens have recently emerged as an increasing global health threat. The escalating incidence of infections caused by MDR *Acinetobacter baumannii, Pseudomonas aeruginosa* and *Klebsiella pneumoniae* has not coincided with endeavours to further antimicrobial drug development and research, potentially placing us on a calamitous path towards the so-called 'post-antibiotic era' (Boucher et al. 2009). A critical need to expand our therapeutic options led to the re-examination of polymyxin antibiotics as a last-line resort (Nation and Li 2009).

A. baumannii has emerged as a very significant pathogen causing life-threatening infections. The remarkable ability of *A. baumannii* to resist dessication (Jawad et al. 1998) and disinfectants (Rajamohan et al. 2009) enhances its potential for rapid spread, contributing to its reputation as a highly troublesome cause of nosocomial outbreaks, particularly in critically-ill and immunocompromised patients (Karageorgopoulos and Falagas 2008). More importantly, multiple intrinsic and acquired mechanisms are intertwined in *A. baumannii*, delivering resistance to an array of antibiotics. These features have culminated in the emergence of extensively drug-resistant strains, that are resistant to all antibiotics including colistin (Peleg et al. 2008). Worryingly, reports of colistin heteroresistance in *A. baumannii* (defined as highly colistin-resistant subpopulations in an isolate that appears susceptible on the basis of minimum inhibitory concentration (MIC)) are also on the rise (Li et al. 2006), emphasizing the need to gain a greater appreciation of the mechanisms of action and resistance to this last-line antibiotic.

The amphipathic nature of colistin is understood to be essential for its antimicrobial activity. Protonation of its five primary amines at physiological pH delivers cationic character, while the *N*-terminal fatty-acyl tail, together with a D-Leucine-L-Leucine domain, conveys hydrophobicity (Storm et al. 1977). Interaction of colistin with the complex Gram-negative outer membrane is believed to be initiated by electrostatic attraction of colistin to the anionic lipid A portion of lipopolysaccharide (LPS), located within the external leaflet of the outer membrane (Hancock and Chapple 1999). Displacement of divalent cations, that normally stabilize the external LPS leaflet, subsequently facilitates the formation of crucial contacts between the hydrophobic colistin domains with lipid A fatty-acyl chains. These hydrophobic forces have been proposed to be the driving force of the interaction (Brandenburg et al. 2002), instigating a disruption of the tightly-packed LPS assembly. In this manner, self-promoted uptake of colistin is mediated across the outer membrane (Hancock and Chapple 1999). Colistin resistance in several Gram-negative species involves lipid A modifications, which diminish the potential for the initial colistin-LPS interaction (Raetz et al. 2007). However, an understanding of the mechanism of colistin resistance in *A. baumannii* has only recently begun to emerge. Differential expression of proteins, and genetic mutations in the two-component PmrAB regulatory system of colistin-resistant *A. baumannii* have been reported (Adams et al. 2009; Fernandez-Reyes et al. 2009). Importantly, the total absence of LPS from the outer membrane of colistin-resistant *A. baumannii*, due to spontaneous mutations in the key lipid A biosynthesis genes, *lpxA, lpxC* or *lpxD*, has recently been revealed as a mechanism of colistin resistance (Moffatt et al. 2010).

Since hydrophobic forces play a vital role in the self-promoted uptake of colistin, the degree of bacterial cell surface hydrophobicity (CSH) may influence the extent to which colistin interactions are able to be established with the outer membrane. CSH remains poorly defined, as traditional methods employed to examine CSH provide indirect estimates based upon bacterial adhesion to model surfaces bearing hydrophobic ligands (Rosenberg et al. 1980; Lachica and Zink 1984), bacterial partitioning between two-phase systems (Miorner et al. 1982), or bacterial co-aggregation in the presence of salt (Lindahl et al. 1981). The lack

of correlation in CSH measurements determined by each of these techniques probably results from the fact that each presents different sensitivities to various outer-membrane constituents which dictate CSH (Dillon et al. 1986). Furthermore, other adhesive forces can interfere with the specific assessment of CSH in these assays.

Alternatively, contact angle measurements offer a reflection of CSH by describing the tendency of a liquid droplet to spread over a solid surface (Busscher et al. 1984). This property is measured by the angle formed at the three-phase boundary following deposition of a water droplet on a bacterial lawn. Hydrophilic surfaces of high wettability yield low contact angles, while the converse is true for hydrophobic surfaces. The contact angle technique has thus been commonly employed to evaluate CSH owing to its simplicity and speed (Busscher et al. 1984). Surface properties such as CSH may alter as a function of bacterial growth phase, due to the dynamic nature of outer-membrane components which continually develop throughout growth (Huisman et al. 1996). In this study our aim was to compare the CSH of colistin-susceptible *versus* -resistant *A. baumannii* at mid-logarithmic and stationary phases, and in response to colistin treatment, using the contact angle technique. Importantly, from these investigations experimental factors influencing contact angles were identified, and methodological considerations necessary to obtain accurate measurements were highlighted.

Materials and Methods

Chemicals

Colistin sulphate was purchased from Sigma-Aldrich (Lot No. 109K1574; Castle Hill, NSW, Australia). A stock solution (1 mgmL^{-1}) was prepared in Milli-Q™ water and filtered through 0.22-μm syringe filters (Sartorius, Melbourne, VIC, Australia), before being stored at 4°C. Under these conditions, colistin has proven stable for at least 1 month (Li et al. 2003).

Bacterial strains

All stock cultures of *A. baumannii* were maintained in tryptone soya broth (TSB; Oxoid, Adelaide, SA, Australia) with 20% glycerol at -80°C. Reference strain ATCC 19606 (colistin MIC 1 mgL^{-1}) was purchased from the American Type Culture Collection (Manassas, VA, USA). Three clinical isolates, namely FADDI-AB013, FADDI-AB014 and FADDI-AB016, each belonging to different clonotypes (Li et al. 2006), were also employed for this investigation (colistin MICs 1 to 2 mgL^{-1}). Paired colistin-resistant strains (colistin MIC > 128 mgL^{-1}) were obtained from each of the above wildtype strains by growth in the presence of 10 mgL^{-1} colistin; these were termed 'R' strains. Additionally, two *A. baumannii* strains derived from the LPS-deficient colistin-resistant strain, 19606R (Moffatt et al. 2010), were investigated to determine the influence of LPS on the CSH of *A. baumannii*. These strains were (i) 19606R+*lpxA,* complemented *in trans* with an intact *lpxA* gene (MIC 1 mgL^{-1}) to restore LPS expression, and (ii) 19606R+V which harbored an empty vector and served as an LPS-deficient control strain (MIC > 128 mgL^{-1}) (Moffatt et al. 2010). Thus in total, contact angle measurements were performed on 10 strains.

For the preparation of mid-logarithmic phase cells, overnight cultures were prepared in cation-adjusted Mueller-Hinton Broth (CaMHB; Oxoid) and used to inoculate fresh medium (1 in 100 dilution), which was then grown at 37°C with shaking (100 rpm) to an OD_{600nm} of between 0.4 and 0.6. For the preparation of stationary-phase cells, cultures were grown overnight. Complemented strains (19606R+*lpxA* and 19606R+V) were grown in the presence of 100 mgL^{-1} ampicillin to maintain selection for the plasmids. Colistin was

excluded from mid-logarithmic and stationary-phase cultures of colistin-resistant cells to avoid potential cell surface modifications.

The effect of colistin treatment on mid-logarithmic cells was investigated at 32 mgL^{-1} in 80 mL of bacterial culture. Treated cultures were incubated in a shaking water bath (37°C, 100 rpm) for 20 min. This volume of culture and treatment duration ensured that a sufficient number of viable cells remained after treatment, to adequately prepare substrata for contact angle measurements. Stationary-phase *A. baumannii* cells were not treated with colistin.

Atomic force microscopic (AFM) imaging

AFM height and amplitude images (10 × 10 μm and 20 × 20 μm) of air-dried bacterial lawns were obtained in tapping mode, using a Dimension 3000™ AFM with a Nanoscope IIIa controller (Digital Instruments, Santa Barbara, CA, USA). Standard silicon nitride tips (Tap300 Budget Sensors®; Bulgaria) were used (125 μm in length, nominal spring constants of 40 $nNnm^{-1}$, and typical resonant frequencies of 300 kHz) to scan samples at a speed of 1 Hz. Large scans (20 × 20 μm) were acquired at a resolution of 256 pixels, while all other images were scanned at 512 pixels. The root-mean-square (RMS) roughness of five separately prepared bacterial lawns was automatically determined from AFM height images (10 × 10 μm) using the Nanoscope® 5.13 software (Digital Instruments, Santa Barbara, CA, USA).

Determination of bacterial contact angles

Contact angles were measured using the sessile-drop method on bacterial lawns (Busscher et al. 1984). Bacteria were isolated by centrifugation (3,000 × *g*, 5 min, 25°C) and washed twice with Milli-Q™ water. This washing protocol has been shown to adequately clean *A. baumannii* cells for surface examination (Moffatt et al. 2010). Cells were subsequently resuspended in Milli-Q™ water to prepare 60 mL of suspension containing ~6×10^8 colony forming units (cfu)mL^{-1}. Bacterial lawns were created by filtering suspensions *via* negative pressure (20 mmHg) through cellulose acetate (Millipore™, North Ryde, NSW, Australia) or polyvinylidene-difluoride membrane filters (PVDF; Millipore™) of 0.22-μm pore size, for 15 min, until the fluid had completely passed through. Wet filters with retained cells were air dried under sterile conditions for ~30 min, then mounted onto glass slides.

A droplet of Milli-Q™ water (11.5 μL) was deposited on bacterial lawns, and images were captured automatically using a KSV Cam 200 (Biolin Scientific, Stockholm, Sweden) contact angle analyser. For each sample, contact angles were measured over ~12 sec; 10 images were acquired immediately following deposition at 0.33-sec intervals, followed by 9 more images at 1-sec intervals. In addition, images were acquired at a final time point of 1 min for strains ATCC 19606 and 19606R at both growth phases. From these images, measurements of contact angle (θ) and droplet volume (μL) were obtained at each time point. Means and standard deviations (SD, n = 12) were calculated from contact angles obtained at separate locations on between 3 and 5 independent bacterial lawns, which were prepared over two different days. Control experiments were conducted on bare PVDF and cellulose acetate filters. The Student's *t*-test, and two-way analysis of variance (ANOVA) with bonferroni post-hoc comparisons, were performed with the GraphPad Prism V5.0 software (GraphPad software, San Diego, USA).

Results

AFM images

AFM images were acquired to verify the nature of the bacterial lawn formed by filtration of untreated ATCC 19606 (colistin-susceptible) and 19606R (colistin-resistant) cultures at mid-

logarithmic phase (Figure 1), illustrating a packed lawn of cells for both strains. Similar results were obtained for stationary-phase cells (data not shown). Rod-shaped colistin-susceptible cells (Figure 1A) were readily differentiated from spherical colistin-resistant cells (Figure 1B), and cellular elongation was observed at stationary phase for both strains (data not shown). The confluent bacterial lawn of colistin-susceptible cells displayed a consistent structure, and exhibited an even distribution across the filter. The surface (Figure 1C) and cross-sectional (Figure 1E) AFM plots of ATCC 19606 displayed only narrow gaps between cells. Greater morphological irregularity was observed for the colistin-resistant strain; AFM images showed that filtration of 19606R cells resulted in a rough and uneven cell distribution across the filter, characterized by clumped cell masses separated by large valleys (Figures 1B, D and F). These observations were supported by RMS-roughness measurements (Table 1) which revealed a significantly rougher topography for the bacterial lawn of colistin-resistant cells (104.2 ± 3.6 nm) in comparison to the colistin-susceptible cell lawns (67.1 ± 3.2 nm) at mid-logarithmic phase ($p < 0.01$). At stationary phase, filtration of both colistin-susceptible and -resistant cells resulted in smoother bacterial lawns in comparison to mid-logarithmic phase cells (Table 1; $p < 0.05$), although this was not visually apparent (data not shown).

Exposure to 32 mgL^{-1} colistin resulted in a smoother surface topography for cells of both phenotypes, without substantially altering morphology (Figure 2). RMS roughness values of colistin-treated bacterial lawns were significantly different (62.0 ± 3.4 and 88.6 ± 2.3 nm, colistin-susceptible and -resistant, respectively) from untreated bacterial lawns (Table 1; $p < 0.05$). However, these differences between colistin treated (Figure 3) and untreated (Figure 1) bacterial lawns were not visually apparent from AFM images.

Contact angles on *A. baumannii* bacterial lawns as a function of time

Considerable swelling of the filter upon contact with the water droplet was demonstrated from control experiments performed on bare cellulose-acetate filters (Figures 4A to C); this was not observed for PVDF filters (Figures 4D to F). Control experiments performed on bare PVDF filters revealed an initial contact angle of 47.3 ± 0.7°, which decreased to 12.5 ± 0.5° after ~12 sec. Following droplet deposition on bacterial lawns of ATCC 19606 (Figure 5A) and 19606R (Figure 5B) prepared on PVDF filters, the contact angle also changed as a function of time over ~12 sec; similar results were obtained for the clinical strains (data not shown). For both phenotypes, the contact angle decreased noticeably immediately after time zero; therefore the final contact angle measurement at ~12 sec has been summarized for all strains in Table 2. Contact angles were also determined 1 min after droplet deposition for ATCC 19606 at mid-logarithmic phase, revealing an angle of 6.10 ± 1.03°. After 1 min, the contact angle for strain 19606R approached zero. A considerable reduction in contact angles after 1 min was also observed for stationary-phase lawns of both strains (10.3 ± 2.14° and 6.32 ± 1.82°, ATCC 19606 and 19606R, respectively). These results indicate that contact angles had failed to stabilize even after 1 min. Contact angles obtained on ATCC 19606 lawns appeared to decline at a similar rate for both growth phases. However, for 19606R lawns, the reduction in contact angle was more rapid at mid-logarithmic phase in comparison to stationary phase (Figure 5). Similar results were detected for the paired colistin-susceptible and -resistant clinical strains (data not shown). After treatment of mid-logarithmic cells with colistin 32 mgL^{-1}, a high contact angle was observed immediately after droplet deposition on lawns of colistin-susceptible strains; within 1 sec contact angles rapidly decreased, before stabilizing to a steady decline which mirrored the trend observed for untreated mid-logarithmic cells (Figure 5). For lawns of colistin-resistant cells, the change in contact angle after colistin treatment followed a similar pattern to that observed for untreated stationary-phase cells (Figure 5).

Droplet volumes on *A. baumannii* bacterial lawns as a function of time

The change in measured droplet volume on bacterial lawns with respect to time (Figures 5C and D, ATCC 19606 and 19606R, respectively) paralleled the change observed for contact angles (Figures 5A and B, ATCC 19606 and 19606R, respectively). Plots of droplet volume *versus* time at both growth phases, and in response to colistin treatment, were almost superimposable for the colistin-susceptible strain ATCC 19606 (Figure 5C) as well as the colistin-susceptible clinical strains (data not shown). In contrast, marked differences were evident for colistin-resistant strains. Figure 5D illustrates that the droplet volume decreased more rapidly on lawns of mid-logarithmic in comparison to stationary phase ATCC 19606R cells. Surprisingly, after colistin treatment of the colistin-resistant strains derived from wildtype clinical strains, the droplet volume appeared to maintain a relatively stable value over the entire ~12 sec duration (data not shown). For 19606R, the rate of volume reduction was similar to that observed for stationary-phase cells (Figure 5D).

Contact angles of *A. baumannii* recorded 0.66 sec after droplet deposition

In order to reduce the possibility of artefactual comparisons that may arise from droplet volume loss, we compared contact angles at a set time (0.66 sec) after deposition of the droplets on bacterial lawns (Table 2). Significantly lower contact angles were displayed overall by the colistin-resistant strains in comparison to the -susceptible strains at both growth phases (ANOVA, $p < 0.05$). However, post-hoc analysis indicated that differences between colistin-susceptible and -resistant phenotypes were not statistically significant for ATCC 19606 at mid-logarithmic phase, nor for paired strain FADDI-AB016 at stationary phase (*t*-test, $p > 0.05$). Both colistin-susceptible and -resistant *A. baumannii* exhibited higher contact angles at stationary phase *versus* mid-logarithmic phase (ANOVA, $p < 0.05$); the magnitude of these differences varied according to the particular strain. The contact angles of colistin-susceptible strains, ATCC 19606 and 19606R+*lpxA*, were not significantly different from each other at either growth phase (*t*-test, $p > 0.05$). The higher contact angle displayed by colistin-resistant strain, 19606R+V in comparison to 19606R (*t*-test, $p < 0.05$), was only observed at stationary phase. Colistin exposure considerably increased the contact angles of lawns of both colistin-susceptible and -resistant cells (ANOVA, $p < 0.05$); this was not significant for strains ATCC 19606 or FADDI-AB013 (*t*-test post-hoc analysis, $p > 0.05$).

Discussion

The external leaflet of the complex Gram-negative outer membrane comprises a tightly-packed LPS layer, which presents a physical barrier to the permeation of numerous antibiotics and contributes to the development of the MDR phenotype (Hancock 1997). Conversely, for the cationic amphipathic colistin molecule, negatively charged phosphorester moieties on lipid A provide an initial binding site for electrostatic interactions to form with the bacterial surface. Subsequently, hydrophobic contacts with lipid A fatty-acyl chains and membrane phospholipids are considered to be crucial to facilitate self-promoted uptake of the peptide (Hancock and Chapple 1999). Alterations to the bacterial outer membrane have been reported to contribute to colistin resistance in *A. baumannii* (Adams et al. 2008; Adams et al. 2009; Fernandez-Reyes et al. 2009), including the complete loss of LPS resulting from mutations in the genes involved in lipid A biosynthesis (namely *lpxA, lpxC* or *lpxD*) (Moffatt et al. 2010). Characterization of the physicochemical cell surface properties, such as CSH, that influence the interaction between colistin and the outer membrane can thus enhance our understanding of the mechanism of colistin action, and the surface changes leading to colistin resistance in this problematic pathogen. The early experimental methods of Busscher et al. (Busscher et al. 1984) have been utilized by numerous researchers to measure contact angles for bacterial CSH examination (Boonaert

and Rouxhet 2000; Ahimou et al. 2001; Anderson et al. 2005; Rivas et al. 2005; Hamadi and Latrache 2008). However, experimental factors that may potentially confound results, such as filter composition and the exact time point at which contact angles are measured, are often not reported in such studies. The lack of experimental detail provided by authors impedes the ability to reliably compare bacterial contact angle data obtained from different laboratories.

Reliable acquisition of contact angle measurements firstly necessitates consideration of the membrane filter composition upon which the bacterial lawn is formed. Numerous commerical membrane filters, composed of various polymers, with different pore sizes exist. Hydrophilic cellulose-acetate membranes are the most common filter cited for bacterial applications (Busscher et al. 1984; Ahimou et al. 2001; Rivas et al. 2005; Hamadi and Latrache 2008). However when these filters were used in the present investigation, considerable swelling of cellulose fibres upon contact with aqueous bacterial suspensions was observed (Figure 4); this hindered an accurate assessment of the baseline from which meaningful contact angles are calculated. Inorganic aluminium oxide (Coldren et al. 2009) or hydrophobic PVDF (Abbasnezhad et al. 2008) membranes have also been used. Hydrophilic Duapore® membranes (a modified form of the hydrophobic PVDF filters) were utilized here, presenting a readily wettable substrate ($\theta_{\sim 12\ sec} = 12.5 \pm 0.5°$), which facilitated the filtration of *A. baumannii* suspensions, and also avoided the swelling phenomenon encountered with cellulose membranes.

Additionally, although the influence of substrate roughness on contact angles has been recognized (Hitchcock et al. 1981; Dang-Vu et al. 2006), the formation of a completely flat and smooth bacterial lawn is an impossible task. Attempts have been made to grow confluent bacterial lawns on agar; however, this method is not applicable to all species (van Loosdrecht et al. 1987). The most common method for the preparation of bacterial lawns involves filtration of a bacterial suspension through porous membrane filters. Published studies have neglected to adequately confirm the nature of the filtered bacterial lawn. Although Busscher et al. (Busscher et al. 1984) acquired scanning electron micrographs to illustrate the uniformity of bacterial packing on the filter surface, it must be noted that electron microscopy requires samples to be fixed, dehydrated and coated with metal. These procedures may obscure an accurate reflection of the native surface, and lead to changes in the bacterial packing arrangement.

Conversely, in the present study, AFM images of *A. baumannii* (Figures 1 to 3) captured without complex dehydration and bacterial manipulation protocols (Dufrene 2004) illustrated considerable differences between colistin-susceptible and -resistant *A. baumannii* lawns (Figure 1). AFM images of 19606R (colistin-resistant) bacterial lawns revealed large crevices (Figure 1). These observations were supported by a higher degree of surface roughness in lawns of colistin-resistant (19606R) cells compared to lawns of colistin-susceptible (ATCC 19606) cells (Table 1; $R_{rms} = 104.2 \pm 3.6$ *versus* 67.1 ± 3.2 nm, 19606R *versus* ATCC 19606, respectively), and may be explained by the tendency for spherical colistin-resistant *A. baumannii* cells to aggregate in clusters and chains (Soon et al. 2009). Filtration of cellular aggregrates would be more likely to lead to an uneven distribution of cells, thus resulting in a bacterial lawn of greater porosity. This finding highlights that the nature of cellular packing is dictated by cellular characteristics (such as shape and physical properties) of the specific bacterial strain under investigation. Our AFM images further suggest that artifactual measurements of contact angle potentially may arise from leakage of the water droplet through the bacterial layer, *via* channels formed between cells.

The effect that dehydration of bacteria-coated filters may impose on the contact angle has been recognized (Busscher et al. 1984) leading to suggestions that filters should be dried for

0 to 90 min before performing measurements; this was proposed to be sufficient to reach a 'plateau' state whereby stable contact angles could be determined (Busscher et al. 1984). Accordingly, in the present study filters were dried for ~30 min. We have demonstrated that contact angles decreased immediately after the water droplet was deposited and failed to attain a plateau state (Figure 5; Table 2), even after 1 min. Changes to the contact angles of both colistin-susceptible and -resistant *A. baumannii* over time, were found to parallel changes in droplet volume as a function of growth phase, and colistin treatment (Figure 5). We therefore propose that the most accurate reflection of CSH was provided by the contact angle at 0.66 sec in this study (Table 2). This time point allowed a sufficient duration for the droplet to settle on the surface, while avoiding misleading results that may have arisen from leakage of the water droplet through the bacterial lawn. Notably, the time point at which contact angles were recorded in previous CSH investigations has often been left undefined.

Lower contact angles, representing lower CSH, observed for colistin-resistant *versus* -susceptible *A. baumannii* at both growth phases may be related to the reduced fimbrial expression previously noted for the colistin-resistant strain (Soon et al. 2009), as the influence of fimbriae on CSH has been described in previous studies for *Acinetobacter* species (Rosenberg et al. 1982; Van der Mei et al. 1991). Additionally, the lack of LPS in the outer membrane of colistin-resistant cells (Moffatt et al. 2010) likely contributes to the reduced CSH of these strains. Indeed, structural variations of LPS have been shown to influence the CSH of Gram-negative bacteria (Camprubi et al. 1992; Burks et al. 2003; Yokota and Fujii 2007). For example, the reduced CSH of deep-rough *P. aeruginosa* mutants bearing truncated LPS structures was correlated with the exposure of phospholipids and lipid A phosphoresters (Yokota and Fujii 2007). The contribution of LPS to CSH was further highlighted from our investigations of complemented strains derived from 19606R. Accordingly, the contact angle of 19606R+*lpxA* (19606R complemented with an intact *lpxA* gene, thus restoring LPS and colistin susceptibility) was not significantly different from that of ATCC 19606 at either growth phase (Table 2; $p > 0.05$). The colistin-resistant strain 19606R+V (19606R strain harbouring empty vector only) showed small contact angle differences from 19606R at stationary phase (Table 2; $p < 0.05$); this result may be attributed in part to ampicillin exposure which was used to maintain selection for the presence of the plasmid during growth of 19606R+V. Exact reasons for this difference remain unknown.

Differences in the contact angles of both colisin-susceptible and -resistant cells were also detected with respect to growth phase, whereby stationary-phase cells exhibited higher contact angles in comparison to cells at mid-logarithmic phase (Table 2; $p < 0.05$). These results, combined with recent reports of cellular elongation (Soon et al. 2009) and surface charge differences detected for stationary *versus* mid-logarithmic phase *A. baumannii* cells (Soon et al. 2011), highlight the continually evolving nature of the outer-membrane structure throughout growth. The resultant structural and compositional differences of the outer membrane give rise to alterations in cell surface properties, which potentially impede the interaction with colistin; these changes may account for the reduced activity of colistin against *A. baumannii* at stationary phase (Poudyal et al.).

In response to treatment with various antimicrobials, a reduction in CSH has been documented for several Gram-negative species (Tateda et al. 1993; McKenney and Allison 1997; Gholia et al. 2004), including *A. baumannii* (Hostacka 1999a; b; 2000). However in the present study, colistin exposure increased the contact angle of both colistin-susceptible and -resistant *A. baumannii* (Table 2; ANOVA, $p < 0.05$). This finding is consistent with the less electronegative surface charge of both phenotypes observed in response to colistin treatment (Soon et al. 2011). For colistin-susceptible cells, these changes in physicochemical properties likely arise from the specific interaction between colistin and LPS, as well as non-

specific interactions with other outer-membrane consituents. In contrast, for colistin-resistant strains deficient in LPS (e.g. 19606R), the increased contact angles and reduced electronegativity after colistin treatment likely result entirely from non-specific binding of colistin to outer-membrane proteins and phospholipids. To the best of our knowledge, our study is the first to reveal that drainage of the water droplet through the porous bacterial lawn bears influence on measurements of bacterial contact angles. Measurements recorded after 0.66 sec on lawns of *A. baumannii* cells revealed a higher CSH for colistin-resistant strains, in comparison to their paired colistin-susceptible strains. These differences in CSH reflect compositional changes to the outer membrane of *A. baumannii,* which affect the binding interaction with colistin and may contribute to colistin resistance. Importantly, investigations of complemented 19606R strains suggest that these outer-membrane alterations involve LPS.

Acknowledgments

The authors would like to thank Ms Jennifer Moffatt (Department of Microbiology, Monash University) for her assistance in providing the *A. baumannii* derivative strains, complemented with and without the *lpxA* gene, for analysis in this investigation.

Funding

This study was supported by a project grant awarded to R.L.N, J.B. and J.L. by the Australian National Health and Medical Research Council (NHMRC). R.L.N and J.L. are supported by research grants from the National Institute of Allergy and Infectious Diseases of the National Institutes of Health (R01A107896 and R01A1079330). J.L. is an Australian NHMRC Senior Research Fellow.

References

Abbasnezhad H, Gray MR, Foght JM. Two different mechanisms for adhesion of Gram-negative bacterium, Pseudomonas fluorescens LP6a, to an oil-water interface. Colloids Surf B Biointerfaces. 2008; 62:36–41. [PubMed: 17997081]

Adams MD, Goglin K, Molyneaux N, Hujer KM, Lavender H, Jamison JJ, MacDonald IJ, Martin KM, Russo T, Campagnari AA, Hujer AM, Bonomo RA, Gill SR. Comparative genome sequence analysis of multidrug-resistant *Acinetobacter baumannii*. J Bacteriol. 2008; 190:8053–8064. [PubMed: 18931120]

Adams MD, Nickel GC, Bajaksouzian S, Lavender H, Murthy AR, Jacobs MR, Bonomo RA. Resistance to colistin in *Acinetobacter baumannii* associated with mutations in the PmrAB two-component system. Antimicrob Agents Chemother. 2009; 53:3628–3634. [PubMed: 19528270]

Ahimou F, Paquot M, Jacques P, Thonart P, Rouxhet PG. Influence of electrical properties on the evaluation of the surface hydrophobicity of *Bacillus subtilis*. J Microbiol Meth. 2001; 45:119–126.

Anderson AJ, Britt DW, Johnson J, Narasimhan G, Rodriguez A. Physicochemical parameters influencing the formation of biofilms compared in mutant and wildtype cells of *Pseudomonas chlororaphis* O6. Water Sci Technol. 2005; 52:21–25.

Boonaert CJP, Rouxhet PG. Surface of lactic acid bacteria: relationships between chemical composition and physicochemical properties. Appl Environ Microbiol. 2000; 66:2548–2554. [PubMed: 10831437]

Boucher HW, Talbot GH, Bradley JS, Edwards JE, Gilbert D, Rice LB, Scheld M, Spellberg B, Bartlett J. Bad bugs, no drugs: no ESKAPE! An update from the Infectious Diseases Society of America. Clin Infect Dis. 2009; 48:1–12. [PubMed: 19035777]

Brandenburg K, Arraiza MD, Lehwark-Ivetot G, Moriyon I, Zahringer U. The interaction of rough and smooth form lipopolysaccharides with polymyxins as studied by titration calorimetry. Thermochimica Acta. 2002; 394:53–61.

Burks GA, Velegol SB, Paramonova E, Lindenmuth BE, Feick JD, Logan BE. Macroscopic and nanoscale measurements of the adhesion of bacteria with varying outer layer surface composition. Langmuir. 2003; 19:2366–2371.

Busscher HJ, Weerkamp AH, van der Mei HC, van Pelt AWJ, DeJong HP, Arends J. Measurement of the surface free energy of bacterial cell surfaces and its relevance for adhesion. Appl Environ Microbiol. 1984; 48:980–983. [PubMed: 6508312]

Camprubi S, Merino S, Benedi J, Williams P, Tomas JM. Physicochemical surface properties of *Klebsiella pneumoniae*. Curr Microbiol. 1992; 24:31–33.

Coldren FM, Palavecino EL, Levi-Polyachenko NH, Wagner WD, Smith TL, Smith BP, Webb LX, Carroll DL. Encapsulated *Staphylococcus aureus* strains vary in adhesiveness assessed by atomic force microscopy. J Biomed Mater Res A. 2009; 89:402–410. [PubMed: 18431772]

Dang-Vu T, Hupka J, Drzymala J. Impact of roughness on hydrophobicity of particles measured by the Washburn method. Physcicochem Probl Miner Process. 2006; 40:45–52.

Dillon JK, Fuerst JA, Hayward AC, Davis GHG. A comparison of five methods for assaying bacterial hydrophobicity. J Microbiol Meth. 1986; 6:13–19.

Dufrene YF. Using nanotechniques to explore microbial surfaces. Nat Rev Microbiol. 2004; 2:451–460. [PubMed: 15152201]

Fernandez-Reyes M, Rodriguez-Falcon M, Chiva C, Pachon J, Andreu D, Rivas L. The cost of resistance to colistin in *Acinetobacter baumannii*: A proteomic perspective. Proteomics. 2009; 9:1632–1645. [PubMed: 19253303]

Gholia N, Toky V, Chhibber S. Effect of antibacterials on surface properties and adhesion to uroepithelial cells in *Klebsiella pneumoniae*. World J Microbiol Biotechnol. 2004; 20:775–779.

Hamadi F, Latrache H. Comparison of contact angle measurement and microbial adhesion to solvents for assaying electron donor-electron acceptor (acid-base) properties of bacterial surface. Colloids Surf B Biointerfaces. 2008; 65:134–139. [PubMed: 18467077]

Hancock RE. The bacterial outer membrane as a drug barrier. Trends Microbiol. 1997; 5:37–42. [PubMed: 9025234]

Hancock REW, Chapple DS. Peptide Antibiotics. Antimicrob Agents Chemother. 1999; 43:1317–1323. [PubMed: 10348745]

Hitchcock SJ, Carroll NT, Nicholas MG. Some effects of substrate roughness on wettability. J Mater Sci. 1981; 16:714–732.

Hostacka A. In vitro effect of imipenem on *Acinetobacter baumannii*. Pharmazie. 1999a; 54:70–72. [PubMed: 9987801]

Hostacka A. Serum sensitivity and surface hydrophobicity of *Acinetobacter baumannii* after postantibiotic effects of quinolones. Biologia. 1999b; 54:283–288.

Hostacka A. Pharmacodynamic parameters of gentamicin and their influence on surface hydrophobicity of *Acinetobacter baumannii*. Ceska Slov Farm. 2000; 49:41–44. [PubMed: 10953442]

Huisman, GW.; Siegele, DA.; Zambrano, MM.; Kolter, R., editors. Morphological and physiological changes during stationary phase. Washington, D. C: ASM Press; 1996.

Jawad A, Seifert H, Snelling AM, Heritage J, Hawkey PM. Survival of *Acinetobacter baumannii* on dry surfaces: comparison of outbreak and sporadic isolates. J Clin Microbiol. 1998; 36:1938–1941. [PubMed: 9650940]

Karageorgopoulos DE, Falagas ME. Current control and treatment of multidrug-resistant *Acinetobacter baumannii* infections. Lancet Infect Dis. 2008; 8:751–762. [PubMed: 19022191]

Lachica RV, Zink DL. Determination of plasmid-associated hydrophobicity of *Yersinia enterocolitica* by a latex particle agglutination test. J Clin Microbiol. 1984; 19:660–663. [PubMed: 6736227]

Li J, Milne RW, Nation RL, Turnidge JD, Coulthard K. Stability of colistin and colistin methanesulfonate in aqueous media and plasma as determined by high-performance liquid chromatography. Antimicrob Agents Chemother. 2003; 47:1364–1370. [PubMed: 12654671]

Li J, Rayner CR, Nation RL, Owen RJ, Spelman D, Tan KE, Liolios L. Heteroresistance to colistin in multidrug-resistant *Acinetobacter baumannii*. Antimicrob Agents Chemother. 2006; 50:2946–2950. [PubMed: 16940086]

Lindahl M, Faris A, Wadstroem T, Hjerten S. A new test based on 'salting out' to measure relative surface hydrophobicity of bacterial cells. Biochim Biophys Acta. 1981; 677:471–476. [PubMed: 7028137]

McKenney D, Allison DG. Influence of growth rate and nutrient limitation on susceptibility of *Burkholderia cepacia* to ciprofloxacin and tobramycin. J Antimicrob Chemother. 1997; 40:415–417. [PubMed: 9338495]

Miorner H, Albertsson PA, Kronvall G. Isoelectric points and surface hydrophobicity of Gram-positive cocci as determined by cross-partition and hydrophobic-affinity partition in aqueous two-phase systems. Infect Immun. 1982; 36:227–234. [PubMed: 7042571]

Moffatt JH, Harper M, Harrison P, Hale JDF, Vinogradov E, Seemann T, Henry R, Crane B, Michael F, Cox AD, Adler B, Nation RL, Li J, Boyce JD. Colistin resistance in *Acinetobacter baumannii* is mediated by complete loss of lipopolysaccharide. Antimicrob Agents Chemother. 2010; 54:4971–4977. [PubMed: 20855724]

Nation RL, Li J. Colistin in the 21st century. Curr Opin Infect Dis. 2009; 22:535–543. [PubMed: 19797945]

Peleg AY, Seifert H, Paterson DL. *Acinetobacter baumannii*: emergence of a successful pathogen. Clin Microbiol Rev. 2008; 21:538–582. [PubMed: 18625687]

Poudyal, A.; Owen, RJ.; Bulitta, JB.; Forrest, A.; Tsuji, BT.; Turnidge, JD.; Spelman, D.; Howden, BP.; Nation, RL.; Li, J. High initial inocula and stationary growth phase substantially attenuate killing of *Klebsiella pneumoniae* and *Acinetobacter baumannii* by colistin. Abstracts of the Forty-eighth Interscience Conference on Antimicrobial Agents and Chemotherapy; Washington, DC. Washington, DC, USA: American Society for Microbiology; 2008. p. Abstract A-1673p. 28

Raetz CR, Reynolds CM, Trent MS, Bishop RE. Lipid A modification systems in Gram-negative bacteria. Annu Rev Biochem. 2007; 76:295–329. [PubMed: 17362200]

Rajamohan G, Srinivasan VB, Gebreyes WA. Biocide-tolerant multidrug-resistant *Acinetobacter baumannii* clinical strains are associated with higher biofilm formation. J Hosp Infect. 2009; 73:287–289. [PubMed: 19762119]

Rivas L, Fegan N, Dykes GA. Physicochemical properties of Shiga toxigenic *Escherichia coli*. J Appl Microbiol. 2005; 99:716–727. [PubMed: 16162222]

Rosenberg M, Bayer EA, Delarea J, Rosenberg E. Role of thin fimbriae in adherence and growth of Acinetobacter calcoaceticus RAG-1 on hexadecane. Appl Environ Microbiol. 1982; 44:929–937. [PubMed: 16346118]

Rosenberg M, Rosenberg E, Gutnick D. Bacterial adherence to hydrocarbons. Microb Adhes Surf. 1980:541–542.

Soon RL, Nation RL, Cockram S, Moffatt JH, Harper M, Adler B, Boyce JD, Larson I, Li J. Different surface charge of colistin-susceptible and -resistant *Acinetobacter baumannii* cells measured with zeta potential as a function of growth phase and colistin treatment. J Antimicrob Chemother. 2011; 66:126–133. [PubMed: 21081544]

Soon RL, Nation RL, Hartley PG, Larson I, Li J. Atomic force microscopy investigation of the morphology and topography of colistin-heteroresistant *Acinetobacter baumannii* strains as a function of growth phase and in response to colistin treatment. Antimicrob Agents Chemother. 2009; 53:4979–4986. [PubMed: 19786595]

Storm DR, Rosenthal KS, Swanson PE. Polymyxin and related peptide antibiotics. Annu Rev Biochem. 1977; 46:723–763. [PubMed: 197881]

Tateda K, Hirakata Y, Furuya N, Ohno A, Yamaguchi K. Effects of sub-MICs of erythromycin and other macrolide antibiotics on serum sensitivity of *Pseudomonas aeruginosa*. Antimicrob Agents Chemother. 1993; 37:675–680. [PubMed: 8494362]

Van der Mei HC, Cowan MM, Busscher HJ. Physicochemical and structural studies on Acinetobacter calcoaceticus RAG-1 and MR-481 - two standard strains in hydrophobicity tests. Curr Microbiol. 1991; 23:337–341.

van Loosdrecht MC, Lyklema J, Norde W, Schraa G, Zehnder AJ. The role of bacterial cell wall hydrophobicity in adhesion. Appl Environ Microbiol. 1987; 53:1893–1897. [PubMed: 2444158]

Yokota, S-i; Fujii, N. Contributions of the lipopolysaccharide outer core oligosaccharide region on the cell surface properties of Pseudomonas aeruginosa. Comp Immunol Microbiol Infect Dis. 2007; 30:97–109. [PubMed: 17182100]

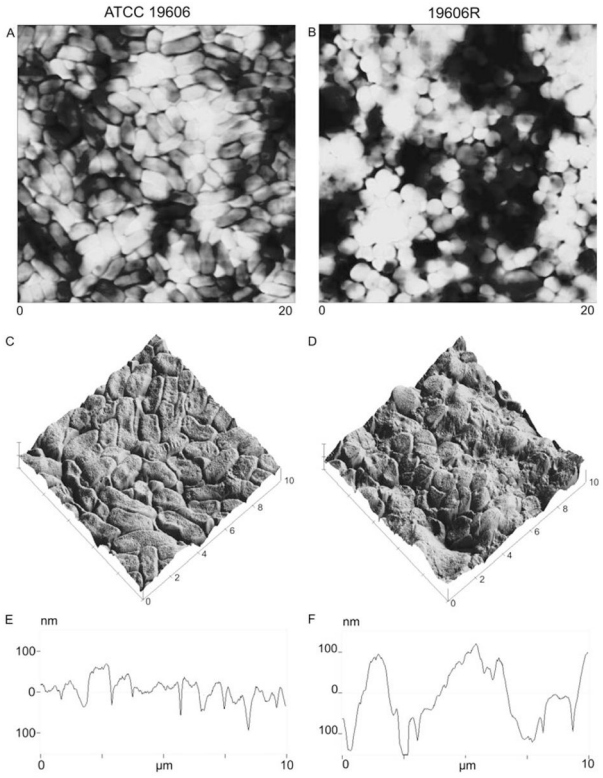

Figure 1.

AFM images of bacterial lawns prepared with ATCC 19606 (panels A, C and E) and 19606R (panels B, D and F) at mid-logarithmic phase. Large scans (panels A and B; 20 × 20 μm) have been presented as height images which provide a reflection of true topographical data by describing changes in sample height; in this manner tall features are illustrated by bright regions, while dark regions portray areas of low sample height. Magnified surface plots (panels C and D; 10 × 10 μm) were constructed from height images, while cross-sections of the 10 × 10 μm plots are illustrated in panel E and F.

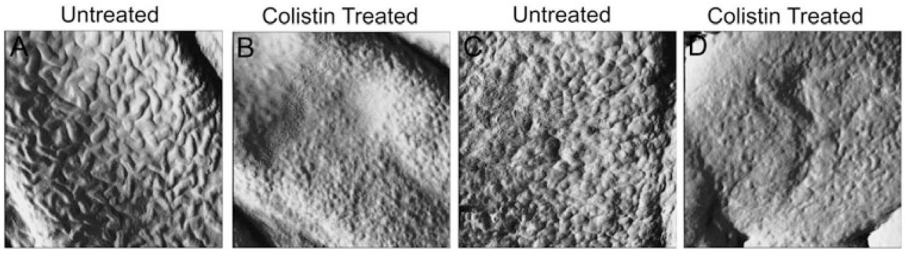

Figure 2.
High magnification AFM amplitude images (1 × 1 μm) of ATCC 19606 (panels A and B) and 19606R (panels C and D) at mid-logarithmic phase, illustrating untreated cells (panels A and C), and cells treated for 20 min with colistin 32 mgL^{-1} (panels B and D).

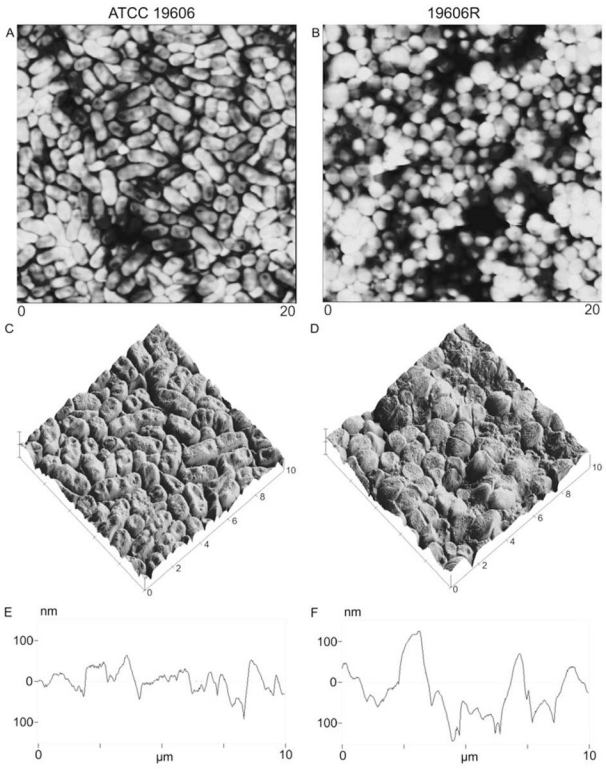

Figure 3.
AFM images of bacterial lawns prepared with ATCC 19606 (panels A, C and E) and 19606R (panels B, D and F) at mid-logarithmic phase treated with 32 mgL^{-1} colistin, presented as: (i) 20 × 20 μm height images (panels A and B); (ii) magnified 10 × 10 μm surface plots, constructed from height images (panels C and D); and, (iii) cross-sections of the 10 × 10 μm surface plots (panels E and F).

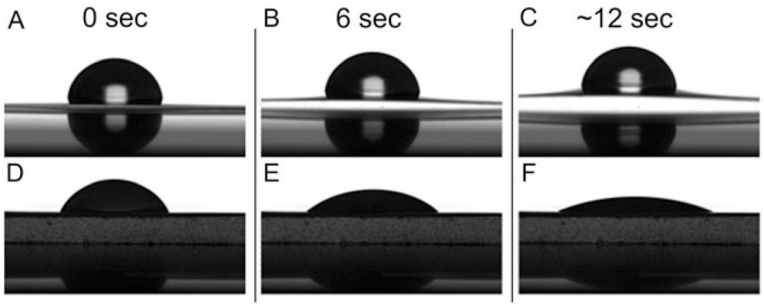

Figure 4.
Images of water droplets deposited on bare cellulose acetate filters (panels A, B and C) and PVDF filters (panels D, E and F) after 0 sec (panels A and D), 6 sec (panels B and E) and 12 sec (panels C and F).

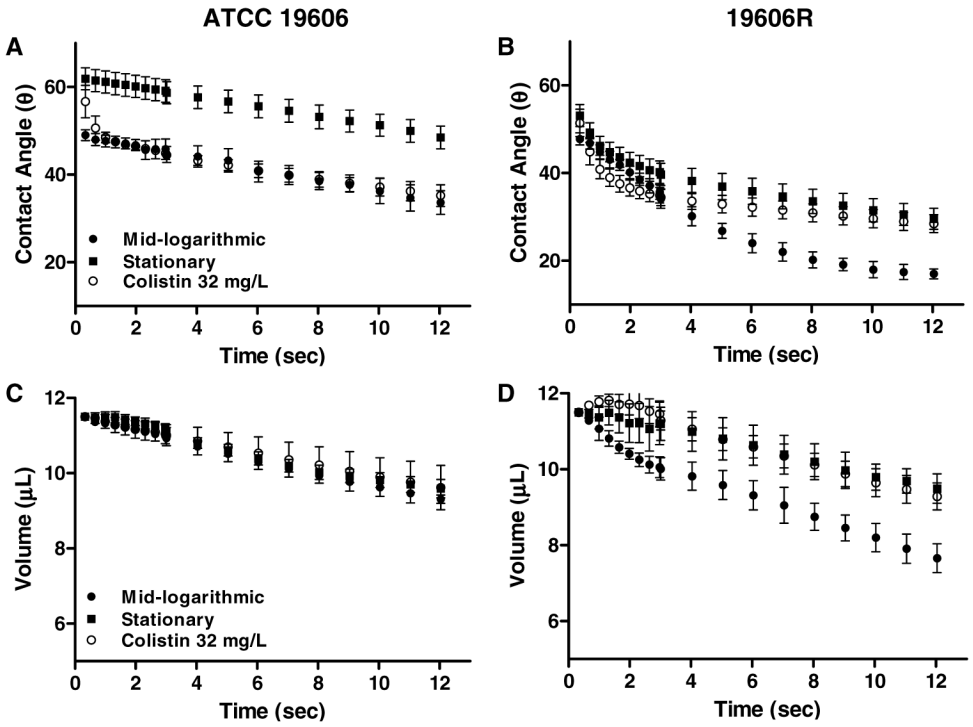

Figure 5.

Change in contact angle (panels A and B, mean ± SD) and droplet volume (panels C and D, mean ± SD) illustrated as a function of time over ~12 sec for ATCC 19606 (panels A and C) and 19606R (panels B and D) at mid-logarithmic and stationary phase, and in response to colistin 32 mgL^{-1} (mid-logarithmic cells).

Table 1

Mean RMS-roughness (nm) ± SD of *A. baumannii* ATCC 19606 and 19606R at mid-logarithmic and stationary phase, and in response to treatment with 32 mgL^{-1} colistin (mid-logarithmic cells). Measurements were determined for five separately prepared bacterial lawns from AFM height images (10 × 10 μm).

	Mid-logarithmic	Colistin 32 mg/L (Mid-logarithmic)	Stationary
ATCC 19606	67.1 ± 3.2[a,b]	62.0 ± 3.4[c]	60.9 ± 2.5[a,b]
19606R	104 ± 3.6[a,b]	88.6 ± 2.3[c]	99.7 ± 2.6[a,b]

[a] Significantly different between colistin-susceptible and -resistant strains for a given growth phase (*T-test,* $p < 0.05$)

[b] Significantly different across growth phases (*T-test,* $p < 0.05$)

[c] Significantly different from untreated mid-logarithmic cells (*T-test,* $p < 0.05$)

Table 2

Contact angles on bacterial lawns of untreated colistin-susceptible and -resistant *A. baumannii*, at mid-logarithmic and stationary phase, and in response to colistin 32 mgL^{-1} (mid-logarithmic cells). Measurements obtained at the initial time-point (t = 0.66 sec) and final time-point (t ~12 sec) are presented.

	Mid-logarithmic		Stationary		Colistin 32 mg/L	
	$\theta_{t = 0.66}$	$\theta_{t \sim 12}$	$\theta_{t = 0.66}$	$\theta_{t \sim 12}$	$\theta_{t = 0.66}$	$\theta_{t \sim 12}$
ATCC 19606	48.0 ± 1.4	33.6 ± 2.7	61.5 ± 2.5	48.5 ± 2.6	50.6 ± 2.8	35.2 ± 2.5
19606R	46.8 ± 1.3	17.0 ± 1.1	49.2 ± 0.6	29.6 ± 2.4	44.9 ± 3.0	28.5 ± 2.1
FADDI-AB013	44.8 ± 1.6	35.5 ± 2.8	51.1 ± 3.9	42.3 ± 2.4	44.5 ± 1.5	36.4 ± 2.9
FADDI-AB013R	41.9 ± 1.6	18.2 ± 1.7	47.4 ± 2.0	28.1 ± 1.9	48.0 ± 2.3	31.9 ± 1.7
FADDI-AB014	40.7 ± 3.0	30.3 ± 2.9	61.4 ± 4.0	50.9 ± 2.0	47.5 ± 3.4	33.2 ± 1.7
FADDI-AB014R	38.8 ± 2.8	16.0 ± 2.3	50.0 ± 2.1	29.3 ± 2.6	43.5 ± 2.2	31.3 ± 2.3
FADDI-AB016	42.6 ± 2.8	34.2 ± 1.5	50.3 ± 2.9	40.9 ± 3.4	46.9 ± 2.2	30.2 ± 2.3
FADDI-AB016R	39.5 ± 1.3	17.8 ± 2.6	50.8 ± 3.2	31.8 ± 3.7	47.4 ± 2.0	37.6 ± 2.6
19606R+*lpxA*	46.9 ± 3.1	29.2 ± 1.1	58.1 ± 1.6	47.9 ± 1.8	51.2 ± 2.1	31.8 ± 1.9
19606R+V	43.1 ± 2.9	20.5 ± 2.7	53.1 ± 1.2	26.2 ± 1.4	50.8 ± 2.3	32.6 ± 2.2